

# The optimization of effective parameters in the leaching of sodium and potassium salts from electric arc furnace dust

Hossein Habibi <sup>a, \*</sup>, Ziaeddin Pourkarimi <sup>a</sup>, Seyed Hossein Hashemi <sup>a</sup>, Dorna Pirouzan, Gholamreza Parvareh <sup>a</sup> and Mahdi Rahimi <sup>a</sup>

<sup>a</sup> Iran Mineral Processing Research Center (IMPRC).

## Article History:

Received: 01 March 2025.

Revised: 10 May 2025.

Accepted: 31 May 2025.

## ABSTRACT

This study optimized water-based leaching parameters for recovering Na and K salts from electric arc furnace (EAF) dust, while enhancing iron content in the residue. Characterization revealed the dust contained 14% Na<sub>2</sub>O, 10.7% K<sub>2</sub>O, and 45.3% Fe<sub>2</sub>O<sub>3</sub>, with particles <15 μm. Response Surface Methodology (RSM) identified temperature (60-70°C) as the most critical factor, achieving 83% Na and 68% K recovery at 25% solid content over 60 minutes. The process enriched the iron grade in the residue by 25% (from 32% to 40% Fe), as validated through large-scale experiments. The method offers dual environmental and economic benefits by minimizing waste and recovering valuable salts.

**Keywords:** *Electric Arc Furnace (EAF) Dust, Sodium and Potassium, Water-based leaching, Environmental sustainability, Waste minimization.*

## 1. Introduction

During the melting and steelmaking process in an electric arc furnace (EAF), a significant amount of dust is generated when charging iron-bearing materials and steel scrap into the furnace. On average, 10 to 20 kg of dust is produced per ton of steel. The large volume of dust creates major challenges. First, transportation and storage require extensive space and result in high costs. Additionally, the current method of storing the produced dust is not a sustainable solution, as it continuously demands more space and poses environmental risks.

Since the introduction of dust collection systems, the steel industry has been dealing with similar materials, such as dust or sludge. Environmental concerns, rising transportation costs, and collection expenses have become critical challenges in this industry. Therefore, from the early days, the reuse of dust and sludge in steel production was considered. However, significant progress was only made when the economic benefits of dust recycling became evident. The first successful attempts involved reusing dust in processes, such as sintering, blast furnaces, converters, and EAFs.

The primary sources of elements entering EAF dust are raw materials, such as scrap and additives. According to previous studies, EAF dust can be categorized based on its chemical composition:

a) Dust from plants that use galvanized scrap, which contains high levels of zinc and lead. These elements contribute to environmental pollution, making their extraction economically valuable. Various products can be obtained, such as crude zinc oxide for further metallurgical refining, iron-rich materials for furnace charging, or useful slag and sponge iron for steelmaking.

b) Dust from alloy and stainless-steel production plants. This type of dust contains significant amounts of nickel and chromium. Several recycling methods for EAF dust have been developed, including raw palletization, PTC, briquetting, Calx briquetting, and direct injection

into the furnace [16]. These methods involve mixing dust with other byproducts, such as mill scale and slag, with or without binders and reductants (e.g., coke or ferrosilicon), forming pellets or briquettes, and reintroducing them into the furnace. Such methods are particularly suitable for alloy steel plants, where the dust contains valuable materials, such as nickel and chromium, which can be effectively recovered in the furnace.

c) Dust from plants that use charge materials with low zinc and lead content but significant amounts of sodium, potassium, and iron. A common method for recycling EAF dust is returning it to the furnace to recover Fe and C. However, this approach reintroduces other elements like potassium, sodium, zinc, and lead into the furnace, which can negatively affect its operation. Recovering sodium and potassium salts is economically beneficial. EAF dust recycling methods often have limitations, such as requiring high capacity for economic feasibility and significant capital investment. Currently, the combination of hydrometallurgical and pyrometallurgical methods for recovering zinc, lead, potassium, sodium, copper, nickel, and other valuable elements on a smaller scale has gained importance. Research on EAF dust recovery in the steel industry has been ongoing for years, with numerous process proposals involving hydrometallurgical, pyrometallurgical, or hybrid approaches. Some solutions suggest integrating EAF dust with other materials at ambient or high temperatures. However, only pyrometallurgical processes (high-temperature metal recovery, HTMR) have achieved significant commercial success, primarily based on modifications of the Waelz process.

Since most steel plants generate dust with high zinc and lead content, most research has focused on processing EAF dust based on its iron and zinc content. In many cases, zinc recovery is the primary driver, as its recovery rate directly affects process economics. Over the past 22 years, many EAF dust recovery projects in the United States have failed, leading to the abandonment of older technical approaches, such as the Waelz process. Economic challenges, lack of technical refinement, and

\* Corresponding author. E-mail address: PSDKHabibi@gmail.com (H. Habibi).

insufficient prior studies have contributed to these failures. Consequently, EAF dust processing remains complex, with several influencing factors, including:

**Particle size and bulk density:** Most particles are smaller than 10 microns, and the bulk density of EAF dust ranges from 1.1 to 2.5 g/cm<sup>3</sup> [17,21]. Due to the fine particle size, agglomeration (pelletization or briquetting) is often required before pyrometallurgical recovery to prevent pneumatic dispersion.

**Zinc content:** The presence of zinc is the main reason for EAF dust recovery. Its concentration significantly impacts process economics.

**Zinc mineralogy:** Zinc in EAF dust typically appears as franklinite (Fe<sub>2</sub>ZnO) and zincite (ZnO). This distinction is crucial in hydrometallurgical processing, as zincite dissolves easily in leaching solutions, whereas franklinite is a stable oxide that requires harsh hydrometallurgical conditions for dissolution.

**Halide compounds:** Most halides exist as potassium and sodium chlorides. Depending on the composition and process, halides can have varying degrees of negative effects.

**Other metals:** EAF dust contains lead, cadmium, chromium, nickel, and copper in varying amounts. In hydrometallurgical processes, these metals often need to be separated before zinc recovery due to technical constraints.

**Copper contamination:** Copper can contaminate the recovered iron from EAF dust, particularly in pyrometallurgical processes where iron recovery occurs alongside zinc extraction.

At Mobarakeh Steel Company, large amounts of Electric Arc Furnace (EAF) dust are produced, requiring collection and recovery to avoid environmental pollution. About 80% of the charge materials are sponge iron, leading to a higher iron content in the dust compared to plants using only scrap. The dust also contains significant levels of zinc, sodium, and potassium, which pose environmental risks. The proposed recovery process involves extracting iron concentrate, recovering sodium and potassium salts, and safely disposing of the remaining waste, reducing iron loss and mitigating environmental concerns.

## 2. Material and methods

The dust sample was prepared by Mobarakeh Steel Company (Isfahan) from the stockpile of collected dust from the electric arc furnaces in the plant and was provided to the researchers. The particle size distribution of the sample was determined using a laser particle size analyzer.

For the precise determination of the total iron content in the sample, wet chemistry methods and titration were employed. To identify the chemical composition of the sample, two representative samples were analyzed using Inductively Coupled Plasma (ICP) and X-ray Fluorescence (XRF) spectroscopy.

For mineralogical studies, X-ray diffraction (XRD) and scanning electron microscopy (SEM) were used.

Leaching experiments were conducted using a water-based system to investigate the influence of critical variables, including temperature, solid content, and leaching time on the recovery of sodium and potassium. The primary objective was to optimize the dissolution of sodium and potassium salts while maximizing the iron content in the residual filter cake. The experimental design was based on response surface methodology (RSM), using the DX7 software to explore the interaction between these variables and determine their optimal levels for efficient leaching. Each test was carried out with 300 grams of the sample using ordinary water in a glass vessel placed on a hot plate, accompanied by mechanical stirring to ensure uniform mixing. The factors chosen (temperature, solid content, and time) were selected based on their known influence on the solubility and leaching kinetics of the target elements.

The pregnant leach solution (PLS) was analyzed by ICP, while the leach residues were characterized using both titration and ICP techniques.

## 3. Results and discussion

### 3.1. Particle size distribution of the sample

The particle size distribution of the sample is shown, and the distribution chart is presented in figure 1. Based on the analysis, the d<sub>80</sub> of the sample was 4 microns, and 100% of the material was finer than 15 microns.

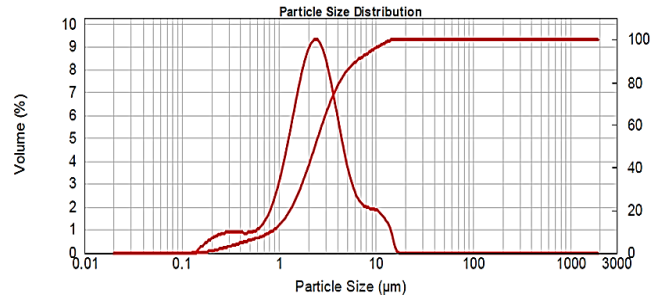


Figure 1. Particle size distribution of the sample.

### 3.2. Chemical characterization of the sample

The total iron content in the sample was found to be approximately 32%. The results of other analyses are presented in Table 1 and Table 2.

Based on the XRF analysis, the sample contained approximately 14% Na<sub>2</sub>O, 7.1% K<sub>2</sub>O, and 32% iron as key valuable components. The sample also contains 2% zinc oxide, 5% calcium oxide, and 2.5% magnesium oxide.

The ICP results indicated that the sample contained 5% potassium and 8.88% sodium, with the zinc content below 0.7%.

### 3.3. Mineralogical characterization of the sample

#### 3.3.1. X-Ray Diffraction (XRD) studies

X-ray diffraction (XRD) analysis revealed that the sample primarily consisted of iron oxide phases, such as magnetite and wüstite, along with phosphosiderite (iron phosphate), sodium carbonate, and diopside. The XRD pattern for the sample is shown in Figure 2.

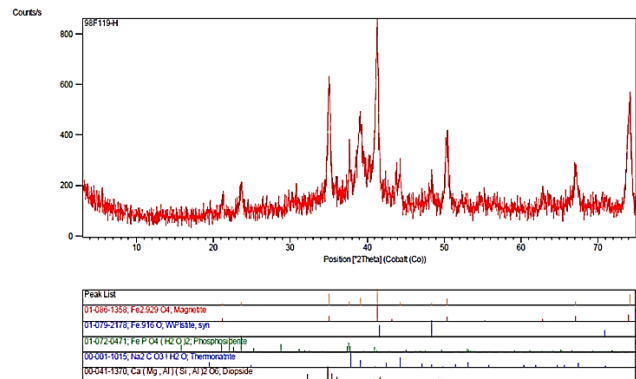


Figure 2. The XRD pattern of the dust sample.

#### 3.3.2. Scanning Electron Microscopy (SEM) studies

Electron microscopy studies were conducted on a polished thin section of the sample. Significant amounts of iron oxides (mainly magnetite, with traces of hematite and goethite) were observed as fine and coarse particles dispersed throughout the sample. In some regions, calcium and potassium were also identified in association with iron oxides. Some iron carbonate, specifically siderite, was identified within the sample. Other minerals and phases identified include a significant amount of pyroxene, some calcite, and minor amounts of silicate

minerals, such as diaspore and biotite. The Energy Dispersive X-ray Spectroscopy (EDS) analysis results obtained from the SEM are provided in the appendix. Most of the oxides are spherical in shape, and dendritic iron solidification particles, fine and coarse oxide particles, siderite, calcite, biotite, as well as calcium, and potassium, containing iron oxides were observed throughout the sample. In Figure 3, one of the EDS analyses obtained by the SEM is shown.

### 3.4. Leaching

The experimental parameters and their respective ranges are summarized in Table 3.

After conducting the leaching experiments, the samples were filtered, with the filter cake undergoing one or two washing steps before being sent for chemical analysis. It is important to note that the fine particle size of the sample posed challenges during filtration, which was a slow

process due to the high specific surface area of the particles. The results from these experiments, focusing on the recovery of sodium and potassium as well as the iron concentration in the filter cake relative to its initial content, are presented in Table 4.

### 3.5. Investigation of potassium dissolution

#### 3.5.1. ANOVA analysis

Based on p-values less than 0.05, the factors influencing potassium dissolution were determined. According to Table 5, only the temperature variable individually affects potassium dissolution. Additionally, there is a minor interaction between temperature and dissolution time. Solid percentage and time alone did not have a significant impact on dissolution within the selected range, but the combined effect of temperature and time is worth investigating.

Table 1. XRF analysis results of the feed sample.

SiO <sub>2</sub> (%)	Al <sub>2</sub> O <sub>3</sub> (%)	CaO(%)	MgO (%)	Fe <sub>2</sub> O <sub>3</sub> (%)	MnO(%)	SO <sub>3</sub> (%)	P <sub>2</sub> O <sub>5</sub> (%)	Na <sub>2</sub> O(%)	K <sub>2</sub> O(%)	ZnO(%)	Cl(%)	Rb <sub>2</sub> O(%)	SUM(%)	LOI(%)
3.62	0.35	5.10	2.54	45.29	0.52	0.56	0.39	14.12	10.74	2.14	0.21	0.12	85.7	14.07

Table 2. ICP analysis results of the feed sample.

Al (%)	As (ppm)	Ca (%)	Cr (ppm)	Cu (ppm)	Fe (%)	K (%)	La (ppm)	Mg (%)
0.41	18.5	4.1	63	72	15	5.01	15	2.21
Mn (ppm)	Na (%)	Ni (ppm)	P (%)	Pb (ppm)	Sr (ppm)	Ti (%)	V (ppm)	Zn (ppm)
1557	8.88	14.5	0.24	616	16.00	0.04	554.00	6917.50

Table 3. Experimental variables for salt leaching.

Variable Name	Unit	Lower Limit	Upper Limit
A: Temperature	°C	25	60
B: Solid content	%	15	25
C: Time	min	30	60

Table 4. The results of the water-based salt leaching experiments with agitation.

Experimental conditions				Products		Solid grade			Solution grade		Results and recovery		
Run	Temp (C)	SR (%)	Time (min)	V (cc)	W (gr)	Fe (%)	Na (%)	K (%)	Na (ppm)	K (ppm)	Na (%)	K (%)	Ratio Fe
1	25	25	60	1010	244.3	37	3.38	6.75	13886	17005	68.7	26.7	1.17
2	40	20	45	1200	233.2	39	2.92	5.55	14988	18840	74.2	42.5	1.22
3	70	20	45	1240	207	42	1.8	3.1	16758	21075	88.8	74.6	1.31
4	40	10	45	1630	235.5	39	2.82	5.13	12264	15280	74.8	46.3	1.23
5	40	20	45	1240	238.8	39	3.03	5.8	15444	19490	72.6	38.4	1.21
6	40	20	45	1190	237.7	39	2.88	5.24	16074	20480	74.1	44.6	1.22
7	25	15	30	1800	224.2	40	2.9	5.56	11430	14025	75.4	44.6	1.25
8	40	30	45	700	209.4	39	2.94	6.12	24150	30160	76.7	43.0	1.23
9	40	20	45	1230	234	40	2.6	4.62	16302	20285	77.0	52.0	1.25
10	13	20	45	1330	238.8	38	3.24	6.5	14130	17025	70.7	31.0	1.19
11	60	25	60	960	216.2	41	2.03	3.25	22254	27600	83.4	68.8	1.28
12	40	20	70	1240	229.2	39	2.64	4.66	16566	20790	77.1	52.5	1.23
13	25	25	30	1050	213.2	39	2.72	5.42	18198	22005	78.0	48.6	1.22
14	60	15	30	1720	208.7	42	2.1	3.57	12804	15860	83.4	66.9	1.30
15	60	15	60	1650	209.7	42	1.86	3.1	13434	16780	85.2	71.1	1.30
16	40	20	20	1230	222.2	40	2.58	4.68	16434	20180	78.3	53.8	1.25
17	40	20	45	1210	218.7	40	2.36	4.72	17034	20444	80.4	54.1	1.24
18	40	20	45	1160	221.2	40	2.58	4.81	17466	21295	78.4	52.7	1.25
19	60	25	30	890	219.2	42	2.63	4.24	22602	28510	78.2	58.7	1.31
20	25	15	60	1850	238.2	38	2.8	5.45	11154	13485	74.736	42.3	1.19

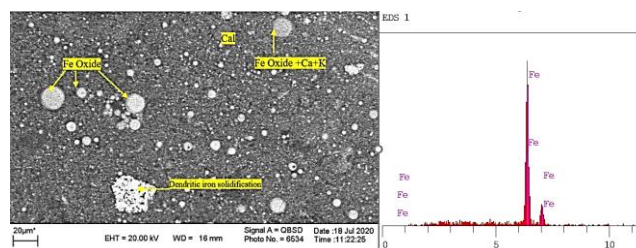


Figure 3. One of the EDS analyses obtained by the SEM.

**Table 5.** ANOVA for potassium dissolution.

Source	Sum of Squares	df	Mean Squares	F value	p-value (Prob > F)
Model	2022.91	2	1011.46	34.25	< 0.0001
A-temp	1870.04	1	1870.04	63.33	< 0.0001
AC	152.87	1	152.87	5.18	0.0361
Residual	501.97	17	29.53	-	-
Lack of Fit	332.13	12	27.68	0.81	0.6451
Pure Error	169.84	5	33.97	-	-
Cor Total	2524.88	19	-	-	-
Statistics					
Std. Dev.	5.43		R-Squared	0.8012	
Mean	46.81		Adj R-Squared	0.7778	
C.V. %	11.61		Pred R-Squared	0.7256	
PRESS	692.81		Adeq Precision	18.702	

Model: The proposed model was significant (p-value < 0.0001) and explained 80.12% of the data variability (R-Squared = 0.8012).

Temperature (A): Temperature had a highly significant effect on potassium dissolution (p-value < 0.0001).

Interaction of Temperature and Time (AC): The interaction between temperature and time also had a significant effect (p-value = 0.0361).

Lack of Fit: The model fitted the data well (p-value = 0.6451).

Effect of Temperature and Time on Potassium Dissolution

Effect of Temperature: Increasing temperature significantly enhanced potassium recovery and dissolution (Figure 5).

Effect of Time: At low temperatures (ambient temperature), increasing time reduced dissolution, whereas at high temperatures, increasing time improved recovery (Figure 6).

**3.5.2. Mathematical model**

Based on the obtained model, the relationship for potassium recovery as a function of temperature and time is defined as:

$$\text{Potassium Recovery (K)} = 50.66 + 12.92 \times A + 4.82 \times A \times C \quad (1)$$

Where:

A: Coded temperature (based on software coding) - C: Coded time (based on software coding).

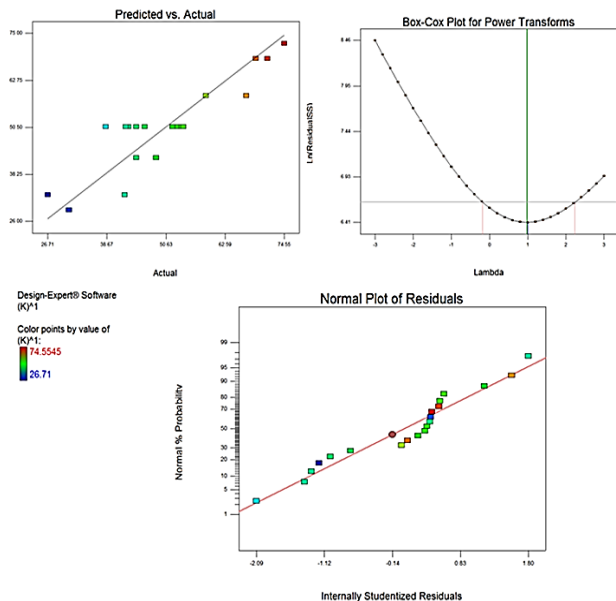


**Figure 4.** BOX-COX plots, normal residuals, and actual vs. predicted values for the experimental design of potassium recovery

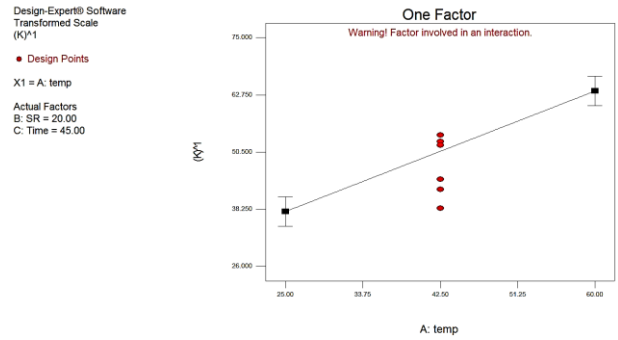


**Figure 5.** The graph of potassium dissolution recovery as a function of temperature.

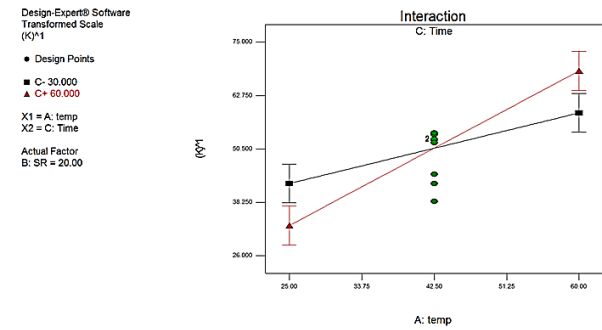


**Figure 6.** The interaction plot of time and temperature for potassium dissolution recovery.

**3.6. Investigation of sodium dissolution**

**3.6.1. ANOVA analysis**

Based on p-values less than 0.05, the factors influencing sodium dissolution were determined. According to Tables 3&4, only the temperature variable individually affected sodium dissolution. Additionally, there was a minor interaction between temperature and dissolution time. Solid percentage and time alone did not have a significant impact on dissolution within the selected range, but the combined effect of temperature and time is worth investigating.

**Table 6.** ANOVA for sodium dissolution.

Source	Sum of Squares	df	Mean Squares	F value	p-value (Prob > F)
Model	1.840E-005	2	9.201E-006	22.54	< 0.0001
A-temp	1.623E-005	1	1.623E-005	39.77	< 0.0001
AC	2.169E-006	1	2.169E-006	5.32	0.0340
Residual	6.938E-006	17	4.081E-007	-	-
Lack of Fit	4.231E-006	12	3.526E-007	0.65	0.7489
Pure Error	2.707E-006	5	5.413E-007	-	-
Cor Total	2.534E-005	19	-	-	-
Statistics					
Std. Dev.	6.39E-04		R-Squared	0.7262	
Mean	0.021		Adj R-Squared	0.694	
C.V. %	3.06		Pred R-Squared	0.6106	
PRESS	9.87E-06		Adeq Precision	14.821	

Model: The proposed model was significant (p-value < 0.0001) and explained 72.62% of the data variability (R-Squared = 0.7262).

Temperature (A): Temperature had a highly significant effect on sodium dissolution (p-value < 0.0001).

Interaction of Temperature and Time (AC): The interaction between temperature and time also had a significant effect (p-value = 0.0340).

Lack of Fit: The model fitted the data well (p-value = 0.7489).

Effect of Temperature: Increasing temperature significantly enhanced sodium recovery and dissolution (Figures 3–5).

Effect of Time: At low temperatures (ambient temperature), increasing time reduced dissolution, whereas at high temperatures, increasing time improved recovery (Figures 3–6).

**3.6.2. Mathematical model**

Based on the obtained model, the relationship for sodium recovery as a function of temperature and time is defined as follows:

$$\text{Sodium Recovery (Na)} - 0.89 = 0.021 - 1.090 \times 10^{-3} \times A - 5.207 \times 10^{-4} \times C \tag{2}$$

Where:

A: Coded temperature (based on software coding)

C: Coded time (based on software coding)

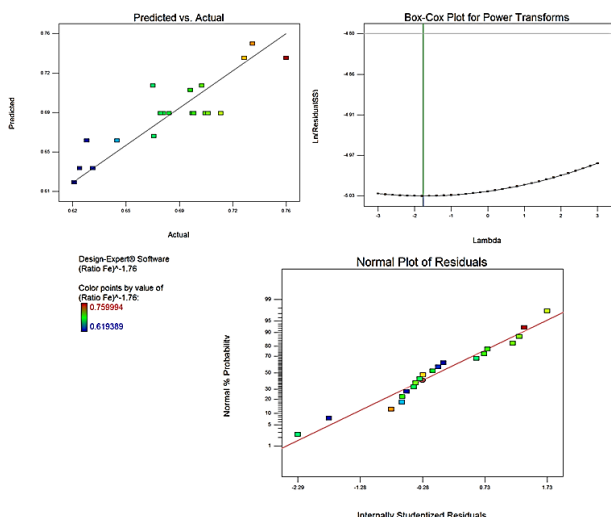


Figure 7. BOX-COX plots, normal residuals, and actual vs. predicted values for the experimental design of sodium recovery.

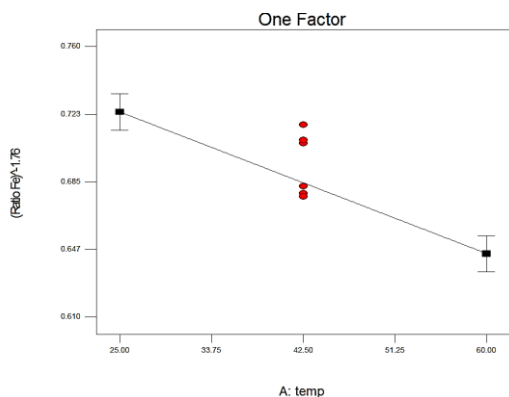


Figure 8. The graph of sodium dissolution recovery as a function of temperature.

**3.7. Optimization**

Based on the obtained results, optimization was performed using software to maximize the recovery of potassium and sodium, as well as to achieve the highest iron ratio in the product relative to the feed, with a desirability of 85%. The optimal conditions were determined to be:

Time: 60 minutes, Temperature: 60–70°C, Solid content: 25%

Under these conditions, the following results were achieved:

Potassium recovery: 68%, Sodium recovery: 83%, Iron grade increase ratio: 1.25

To validate the proposed model, a verification experiment was conducted under conditions similar to Experiment No. 11 in Tables 3–2. The results were consistent, with potassium recovery at approximately 68.8%, sodium recovery at 83%, and an iron grade increase ratio of 1.28.

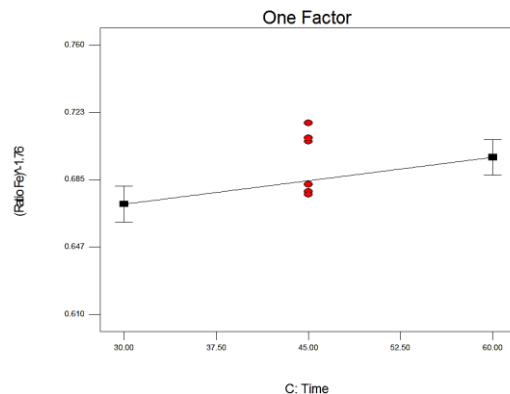


Figure 9. The interaction plot of time and temperature for sodium dissolution recovery.

**3.8. Large-scale leaching experiment**

A large-scale leaching experiment was conducted using 20 kg of the sample under the optimized laboratory conditions. The sample was washed with 60 liters of water at a temperature above 60°C for 1 hour. The chemical analysis of the solid residue is presented in Table 7, and the analysis of the resulting solution is provided in Table 8.

Table 7. The ICP analysis of the washed solid residue.

Al (%)	Bi (ppm)	Ca (%)	Ce (ppm)	Cr (ppm)	Cu (ppm)	K (%)	La (ppm)	Mg (%)	Mn (ppm)
0.53	256	5.28	162	70	398	1.75	37	2.67	3300
Na (%)	Ni (ppm)	P (%)	Pb (ppm)	S (%)	Fe (%)	Sr (ppm)	Ti (%)	V (ppm)	Zn (ppm)
1.94	37	0.36	739	0.35	41	49	0.87	622	14233

Table 8. The ICP Analysis of the Leach Solution.

Al (ppm)	As (ppm)	Ba (ppm)	Ca (ppm)	Cr (ppm)	Fe (ppm)	K (ppm)
27.53	11	0.01	3.09	29.02	0.85	19100
Mg (ppm)	Mo (ppm)	Na (ppm)	P (ppm)	Sb (ppm)	Si (ppm)	V (ppm)
0.73	0.98	21500	87.26	0.18	70.64	120.8

Large-scale experiments demonstrated the feasibility of scaling up the process, with significant recovery of sodium and potassium and the enrichment of iron in the solid residue.

**4. Conclusions**

This study investigated the recovery of sodium and potassium salts from electric arc furnace (EAF) dust generated during steelmaking processes at Mobarakeh Steel Company. The research focused on optimizing the leaching process to maximize the dissolution of sodium and potassium while increasing the iron grade in the solid residue. Analysis of the EAF dust revealed that the sample contained significant amounts of sodium (14% Na<sub>2</sub>O), potassium (10.7% K<sub>2</sub>O), and iron (45.3% Fe<sub>2</sub>O<sub>3</sub>), with a particle size distribution showing 100% of

particles finer than 15 microns ( $d_{80} = 4$  microns). Water-based leaching experiments, optimized using response surface methodology (RSM), demonstrated that temperature is the most influential factor in sodium and potassium recovery. Higher temperatures (60–70°C) with a solid content of 25% over 60 minutes achieved recovery rates of 83% for sodium and 68% for potassium. The process increased the iron grade in the residue by a factor of 1.25, making it suitable for further processing. The optimized conditions (60 minutes, 60–70°C, 25% solid content) were validated through large-scale experiments, confirming the model's reliability. The results demonstrated the feasibility of scaling up the process for industrial applications. The proposed method reduces environmental risks by minimizing waste and offers economic benefits through the recovery of valuable salts and enhanced iron grade.

## Acknowledgments

The authors would like to express their sincere gratitude to Mobarakeh Steel Company of Isfahan and the Iran Mineral Processing Research Center (IMPRC) for their support and collaboration throughout this research.

## References

- [1] Aune, J.: "Electric Arc Furnace Dust Symposium", 1991, Pittsburgh, USA.
- [2] Buzin, P.J.W.K., Heck, N.C., Vilela, A.C.F.: "EAFD – A Thermodynamic Analysis and Classification of Dust Types", Proceedings of the 45th ggSteelmaking Seminar – International, 2014.
- [3] Chaubad, P.C., Okeefe, T.J.: "Ironmaking and Steelmaking", 2 (1982) No.6, P.258-260.
- [4] Chung-Lee Li, Shing, M.: "ISIJ International", 33 (1993) No.2, P.248-290.
- [5] Cruells, M., Rocu, A., Nunez, C.: "Hydrometallurgy", 31 (1992) No. 3, P.213-231.
- [6] Hagni, A.M., Hagani, R.D., Demars, C.: "Journal of Metals", 43 (1991) No. 4, P.28-30.
- [7] Hopkins, D.W., Johnson, W., Davies, R.: "Ironmaking and Steelmaking", 2 (1975) No.1, P.25-29.
- [8] International Iron and Steel Institute (IISI): "The Management of Steel Industry By-Product and Waste", 1987.
- [9] Kawala: "Proceedings of International Symposium on Extractive Metallurgy of Zinc", 14-19 1985, Tokyo, Japan, P.759-805.
- [10] Kotrota, N.I.: "Electric Arc Furnace Dust Symposium", 1989, Pittsburgh, USA.
- [11] Lightfoot, R.: "Electric Arc Furnace Dust Symposium", 1991, Pittsburgh, USA.
- [12] Medonnell, C.F., Triger, D.R., Argent, B.: "Ironmaking and Steelmaking", 16 (1989) No. 6, P.435-445.
- [13] Nyirenda, R.L.: "The Processing of Steelmaking Flue Dust: A Review", Minerals Engineering, 1991;4(7-11):1003-25.
- [13] Pedro Jorge Walburga Keglevich de Buzina, Nestor Cezar Heck, Antônio Cezar Faria Vilela: "EAF Dust: An Overview on the Influences of Physical, Chemical and Mineral Features in Its Recycling and Waste Incorporation Routes", Journal of Materials Research and Technology, 2017;6(2):194-202.
- [14] Pickles, C.A.: "Thermodynamic Analysis of the Selective Chlorination of Electric Arc Furnace Dust", Journal of Hazardous Materials, 2008;166(2-3):1030-42.
- [15] Pirect, N.I. Muler, D.: "Criteria for the Selection of Recycling Process for Low Zinc Containing Residuals from the Iron/Steel Industry", in Residues and Effluents-Processing for Environmental Considerations Conference. 5 Mar 1992, The Minerals, Metals & Materials Society. San Diego, California, P.613-646.
- [15] Pustrip, J.F.: "Electric Arc Furnace Dust Symposium", 1991, Pittsburgh, USA.
- [16] Shahverdi, H.R., Mohammad, M.: "Investigation of Steelmaking Dust in Electric Arc Furnace", Ministry of Mines and Metals, Alloy Steel Company of Iran, Steel Symposium 75, 3-5 Mehr 1375, Materials Engineering Faculty, Isfahan University of Technology.
- [17] Southwick, L.M.: "Still No Simple Solution to Processing EAF Dust", Steel Times International, 2010, p.43-45. Available from: [www.steeltimesint.com/content/images/features/EAF\\_dustMar10.pdf](http://www.steeltimesint.com/content/images/features/EAF_dustMar10.pdf) [cited 15.07.13].
- [18] Svoboda, J.M.: "AFS Transaction", vol 99 (1991), p.405-409.
- [19] West, N.G.: "Iron and Steel International", (1976), June, P.173-185.